

Channel Selection of Ultracold Atom-Molecule Scattering in Dynamic Magnetic Fields

Hanwei Yang,^{1,*} Zunqi Li,^{1,*} Songbin Zhang,² John L. Bohn,³ Lushuai Cao,⁴

Shutao Zhang,¹ Gaoren Wang,^{5,†} Haitan Xu,^{6,7,‡} and Zheng Li,^{1,8,9,§}

¹*State Key Laboratory for Mesoscopic Physics and Collaborative Innovation Center of Quantum Matter, School of Physics, Peking University, Beijing 100871, China*

²*Department of Physics, Shaanxi Normal University, Xi'an 710119, China*

³*JILA, University of Colorado, Boulder, Colorado 80309, USA*

⁴*MOE Key Laboratory of Fundamental Physical Quantities Measurement & Hubei Key Laboratory of Gravitation and Quantum Physics, PGMF and School of Physics, Huazhong University of Science and Technology, Wuhan 430074, China*

⁵*School of Physics, Dalian University of Technology, Dalian 116024, China*

⁶*Shenzhen Institute for Quantum Science and Engineering, Southern University of Science and Technology, Shenzhen 518055, China*

⁷*School of Physical Sciences, University of Science and Technology of China, Hefei 230026, China*

⁸*Collaborative Innovation Center of Extreme Optics, Shanxi University, Taiyuan, Shanxi 030006, China*

⁹*Peking University Yangtze Delta Institute of Optoelectronics, Nantong, China*

 (Received 15 March 2022; revised 2 May 2022; accepted 19 May 2022; published 27 June 2022)

We demonstrate that final states of ultracold molecules by scattering with atoms can be selectively produced using dynamic magnetic fields of multiple frequencies. We develop a multifrequency Floquet coupled channel method to study the channel selection by dynamic magnetic field control, which can be interpreted by a generalized quantum Zeno effect for the selected scattering channels. In particular, we use an atom-molecule spin-flip scattering to show that the transition to certain final states of the molecules in the inelastic scattering can be suppressed by engineered coupling between the Floquet states.

DOI: [10.1103/PhysRevLett.129.013402](https://doi.org/10.1103/PhysRevLett.129.013402)

The ancient Zeno's arrow paradox states that a flying arrow seems not moving when being observed at any single instant. Some decades ago, it was generalized to the quantum Zeno effect (QZE) which states that one can freeze the evolution of a quantum system by frequent measurements. In this context, Kofman and Kurizki (KK) proposed dynamical control of quantum mechanical decay based on continuous modulation of the coupling to an ancillary system [1,2], which was proved to be equivalent to the concept of "frequent observation" of the system since a measurement is nothing but an interaction with an external system playing the role of apparatus [3,4], and the decay is suppressed owing to a coupling modulation. Such effects have been broadly applied in quantum optics, quantum computation, and quantum communication [5–9].

In this Letter we show that the quantum Zeno effect can also be realized in the atom-molecule scattering process manipulated by time-dependent external fields. It has always been a major goal in molecular dynamics to control the scattering via external fields [10–13]. This goal has stimulated the development of quantum control of molecular processes [14–17], which leads to amazing results in unimolecular chemical reactions [18,19]. Attaining control over molecular collisions with simple physical pictures, however, is a big challenge due to the complexity of the molecular interaction involving the rotational, translational, and spin degrees of freedom of the system. Recent theory and experiments [20–24] demonstrated that inelastic

collisions in an ultracold gas of molecular mixtures can be effectively tuned by applying a static magnetic field. Furthermore, enhancing the rate of specifically chosen reaction channels stimulated the development of quantum control schemes such as optimal control and coherent control [14,25].

Despite the many studies on tuning the scattering with static magnetic field, the effects of time-dependent magnetic fields on the post-scattering state distributions and branching ratios for the different reaction channels remain largely unknown. For transitions between bound states, it was found that the transition rate can be suppressed via the modulation of external field [26]. In addition, previous studies proposed that the single-frequency magnetic field can enhance the pairwise interactions resonantly for the ultracold collisions [27,28]. However, for the more general case of inelastic scattering, the simple physical picture of quantum control with an external field of single frequency may not work due to the complexity of the final state spectrum.

Here, we develop a multifrequency Floquet coupled channel (MFF-CC) method to study the atom-molecule inelastic scattering controlled with a time-dependent magnetic pulse train, and demonstrate a selective quantum Zeno effect (SQZE) for selected scattering channels. Kofman *et al.* have proved that the effect on decay rate induced by frequent observations can be expressed as the overlap between the transition probability $G(E)$ and the spectral

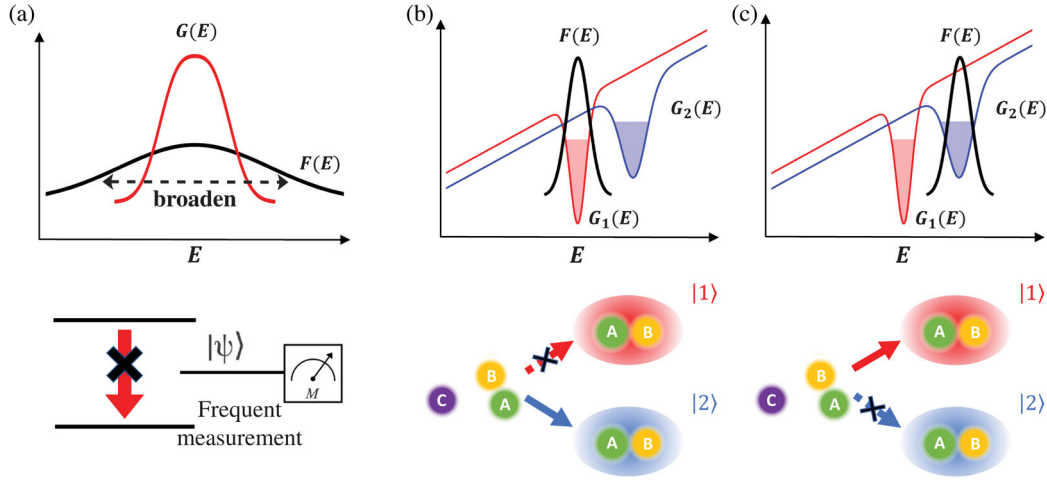


FIG. 1. Schematic diagram of the selective quantum Zeno effect in the collision between a molecule AB and an atom C . The frequent-observation-induced quantum Zeno effect is reflected by reduced overlap between the transition probability $G(E)$ and spectral modulation function $F(E)$ as the latter is broadened by frequent measurements (a) [2]. In (b) and (c), the red and blue curves represent the transition probabilities $G_f(E)$ from an initial state of the molecule to two different final states $|f\rangle$ ($f = 1, 2$) after the collision as a function of final state energy E , which have minima at different energies. The spectral modulation function $F(E)$ reflects the temporal variation of eigenenergies of the collision complex induced by external field, and its overlap with the scattering probability $G_f(E)$ determines the cross section for transition to the final state $|f\rangle$, i.e., $\sigma_f = \int F(E)G_f(E)dE$. By choosing a proper external field, we can make the distribution of $F(E)$ coincide with one of the valleys of $G_f(E)$, and the cross section of the corresponding channel is then suppressed. In this manner, we can engineer the spectral modulation function to suppress the yield of final state $|1\rangle$ [red part in the lower panel of (b)] or $|2\rangle$ [blue part in the lower panel of (c)].

modulation function $F(E)$, i.e., $\int F(E)G(E)dE$, thus QZE is equivalent to suppressing the decay rate by, e.g., broadening $F(E)$ [see Fig. 1(a)] [2]. Further exploiting this equivalence, we propose the SQZE for the inelastic scattering, which is schematically illustrated in Figs. 1(b) and 1(c). Our theory permits reverse engineering of Floquet control fields with a clear physical picture, and we can determine the waveform of a magnetic pulse train to selectively suppress one of the scattering channels. Numerically, we incorporate multifrequency Floquet theory into coupled channel calculation to characterize the interaction of the collision complex with the magnetic pulse train, and show with a concrete example that the cross sections of different spin-flip channels of the scattering between $^{17}\text{O}_2$ and ^3He at ultracold temperatures can be precisely controlled. This work provides new degrees of freedom to realize channel selection in ultracold inelastic scattering, and the underlying dynamic control method can be applied to a broad range of collision processes including resonant magneto-association [29,30] and multichannel reactive collision [12].

We begin by outlining the multifrequency Floquet quantum control approach used to treat the interaction of collision complex with the magnetic pulse train. For collisions between an oxygen molecule in its ground electronic state $^3\Sigma_g^-$ and a helium atom in pulsed magnetic field, the Floquet Hamiltonian in the space-fixed reference (setting $\hbar = 1$) is

$$\hat{H}_F = -\frac{1}{2\mu R} \frac{\partial^2}{\partial R^2} R + \frac{\hat{l}^2}{2\mu R^2} + \hat{V}(\mathbf{R}, \mathbf{r}) + \hat{H}_{\text{as}} - i \frac{\partial}{\partial t}, \quad (1)$$

where R is the atom-molecule separation, μ is the reduced mass of the collision complex, \hat{l} is the orbital angular momentum of the collision, r is the internuclear distance between oxygen atoms in the diatomic molecule, and $\hat{V}(\mathbf{R}, \mathbf{r})$ is the interaction potential between the atom and the molecule [31]. The asymptotic Hamiltonian \hat{H}_{as} depicts the rotational motion of the oxygen molecule and the interaction between its electron spin S and the time-dependent magnetic field $B(t)$ through the Zeeman effect. The total wave function of the collision complex can be expressed in a direct product basis, $\Psi = R^{-1} \sum_{\alpha K l m_l} \mathcal{F}_{\alpha K}^{l m_l}(R) |\alpha K\rangle |l m_l\rangle$, where m_l denotes the projection of \hat{l} on the magnetic field axis, $|\alpha K\rangle$ is the eigenstate of the asymptotic Floquet Hamiltonian $\hat{H}_{\text{asF}} = \hat{H}_{\text{as}} - i(\partial/\partial t)$, α indicates different channels, and K is the index of Floquet eigenstates.

The magnetic pulse train $B(t) = B_0 + \mathcal{B}(t)$ consists of a set of oscillatory magnetic fields of different frequencies. Here B_0 is the static part and $\mathcal{B}(t) = \sum_{n \geq 1} a_n \cos(n\omega_B t)$ is the pulsed field containing multiple Fourier components of frequencies $n\omega_B$. We expand the asymptotic Floquet eigenstates in Fourier basis as $|NSJM_J K\rangle = \sum_n W_{NSJM_J K, n} |NSJM_J n\rangle$, where \hat{N} is the rotational angular momentum, $\hat{J} = \hat{N} + \hat{S}$, M_J is the projection of J on the

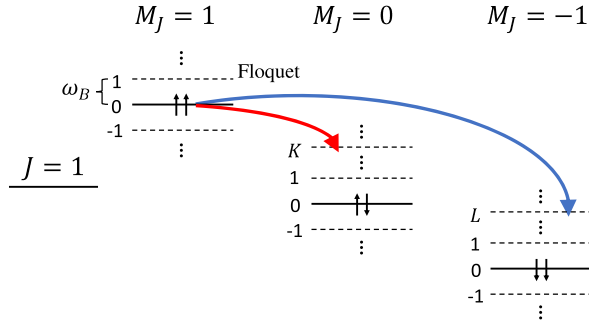


FIG. 2. The mechanism of the spin flipping process $|1, 0\rangle \rightarrow |0, K\rangle$ (red arrows) and $|1, 0\rangle \rightarrow |-1, L\rangle$ (blue arrows). The dashed lines indicate the series of Floquet levels with energy spacing of ω_B .

magnetic field axis, and $|n\rangle$ satisfies $\langle t|n\rangle = e^{in\omega_B t}$. The coupling between different N s, J s is weak (the fine structure coupling is small compared to the rotational separation) and N , J can be considered approximately as good quantum numbers, so that we use $|NSJM_J\rangle$ to label the scattering channel α [20]. We use the coupled angular momentum basis in the calculation, and the MFF-CC method can also be performed in the uncoupled basis $|NM_N\rangle|SM_S\rangle$ [32] (see Supplemental Material [33] for details). The asymptotic Floquet Hamiltonian matrix can be expressed as $\langle \alpha n | \hat{H}_{asF} | \beta m \rangle = H_{\alpha\beta}^{n-m} + n\omega_B \delta_{\alpha\beta} \delta_{nm}$, where $H_{\alpha\beta}^{n-m}$ are Fourier components of H_{as} , i.e., $\langle \alpha | \hat{H}_{as} | \beta \rangle = \sum_{k=-\infty}^{\infty} H_{\alpha\beta}^k e^{ik\omega_B t}$. The Floquet energy difference between $|\alpha K\rangle$ and $|\alpha, K+L\rangle$ is $L\omega_B$. The total wave function is calculated using the MFF-CC formalism (see Ref. [33] for details).

We now apply the MFF-CC method to study the effects of magnetic pulse train on the spin-flip scattering channels ${}^3\text{He} + {}^{17}\text{O}_2(M_J = 1) \rightarrow {}^3\text{He} + {}^{17}\text{O}_2(M_J = 0, -1)$ at temperature $\sim 1 \mu\text{K}$, which produce different final spin states of $M_J = 0$ and $M_J = -1$. A schematic diagram in Fig. 2 demonstrates the transition channels between initial and final states while the laboratory projection of total angular momentum $M_J + m_j$ is conserved. We drop N , S , J as they remain unchanged for the initial and final states of the collision considered in this work, and abbreviate $|NSJM_J K\rangle$ as $|M_J K\rangle$. We focus on the inelastic collision for the initial spin-up state $|1, 0\rangle$. The two spin-flip channels are $|1, 0\rangle \rightarrow |0, K\rangle$ and $|1, 0\rangle \rightarrow |-1, L\rangle$. We denote the Zeeman energies of $|M_J = 0, 0\rangle$ and $|M_J = \pm 1, 0\rangle$ by e_0 , e_{\pm} . For the magnetic field considered in this work, $e_+ - e_0$ and $e_0 - e_-$ are equal and proportional to B_0 , and we can set $e_0 = 0$ and $e_{\pm} = \pm hB_0$, where the coefficient $h = 1.6847 \times 10^{-27} \text{ J/G}$ for the ${}^{17}\text{O}_2$ molecule in ${}^3\Sigma_g^-$ state. We denote the incident kinetic energy as E_{in} , and the kinetic energies after inelastic collision are $E_{out} = E_{in} + hB_0 - K\omega_B$ and $E_{out} = E_{in} + 2hB_0 - L\omega_B$ for the $|1, 0\rangle \rightarrow |0, K\rangle$ and $|1, 0\rangle \rightarrow |-1, L\rangle$ channels, respectively. In the laboratory frame the asymptotic energies of states with $M_J = 0, \pm 1$ are $0, \pm hB(t)$, thus the total energy

before the collision is $E_{in} + hB_0 + h\mathcal{B}(t)$ and after the collision changes to $E_{in} + hB_0 - K\omega_B$ or $E_{in} + hB_0 - h\mathcal{B}(t) - L\omega_B$ for the scattering channel $|1, 0\rangle \rightarrow |0, K\rangle$ or $|1, 0\rangle \rightarrow |-1, L\rangle$.

To show the selective quantum Zeno effect, we model the inelastic scattering as transitions from initial state $|1, 0\rangle$ to a series of final states $\{|0, K\rangle\}$ and $\{|-1, L\rangle\}$ of ${}^{17}\text{O}_2$ molecules with the effective Hamiltonian $\hat{H}(t) = \hat{H}_0 + \hat{H}_{int}$ [1], where

$$\begin{aligned} \hat{H}_0 &= (hB_0 + h\mathcal{B}(t))|1, 0\rangle\langle 1, 0| \\ &+ \sum_K (hB_0 - K\omega_B)|0, K\rangle\langle 0, K| \\ &+ \sum_L (hB_0 - h\mathcal{B}(t) - L\omega_B)|-1, L\rangle\langle -1, L| \end{aligned} \quad (2)$$

with the constant E_{in} neglected, and

$$\hat{H}_{int} = \sum_K g_0 |1, 0\rangle\langle 0, K| + \sum_L g_{-1} |1, 0\rangle\langle -1, L| + \text{H.c.} \quad (3)$$

is the effective coupling between the initial state of molecule $|1, 0\rangle$ and the final states $\{|0, K\rangle\}$, $\{|-1, L\rangle\}$, where the coupling strengths g_0 and g_{-1} are functions of the exit kinetic energy E_{out} .

The wave function of the system at time t can be approximated as

$$\begin{aligned} \Psi(t) &= c_1(t) e^{-ihB_0 t - i \int_0^t h\mathcal{B}(t') dt'} |1, 0\rangle \\ &+ \sum_K c_{0,K}(t) e^{-i(hB_0 - K\omega_B)t} |0, K\rangle \\ &+ \sum_L c_{-1,L}(t) e^{-i(hB_0 - L\omega_B)t + i \int_0^t h\mathcal{B}(t') dt'} |-1, L\rangle, \end{aligned} \quad (4)$$

with the initial condition $c_1(0) = 1$, $c_{0,K}(0) = 0$, $c_{-1,L}(0) = 0$. Because transitions to $|1, M\rangle$ for $M \neq 0$ are of higher order, the amplitude $c_{1,M}$ is negligible in Eq. (4). For the spin-flip transition $|1, 0\rangle \rightarrow |0, K\rangle$, we introduce a modulation function $\varepsilon_0(t) = \exp[-i \int_0^t h\mathcal{B}(t') dt']$ and expand it in Fourier series $\varepsilon_0(t) = \sum_K \lambda_{0,K} e^{iK\omega_B t}$. Similarly we introduce $\varepsilon_{-1}(t) = \exp[-i \int_0^t 2h\mathcal{B}(t') dt'] = \sum_L \lambda_{-1,L} e^{iL\omega_B t}$ for $|1, 0\rangle \rightarrow |-1, L\rangle$ transition. This temporally modulated system can be treated perturbatively [1, 3, 34], which gives the transition rates $\partial_t |c_{0,K}(t)|^2 = 2\pi |\lambda_{0,K}|^2 |g_0(E_{out})|^2$ and $\partial_t |c_{-1,L}(t)|^2 = 2\pi |\lambda_{-1,L}|^2 |g_{-1}(E_{out})|^2$ (see Supplemental Material [33] for details). We introduce the spectra of modulation functions for final states

$$F_{M_J}(E) = \sum_K |\lambda_{M_J, K}|^2 \delta(E - [(1 - M_J)hB_0 - K\omega_B]), \quad (5)$$

which account for the modulation of exit energies E_{out} . Let $\sigma_0 = \sum_K \sigma_{0,K}$ and $\sigma_{-1} = \sum_L \sigma_{-1,L}$ denote total

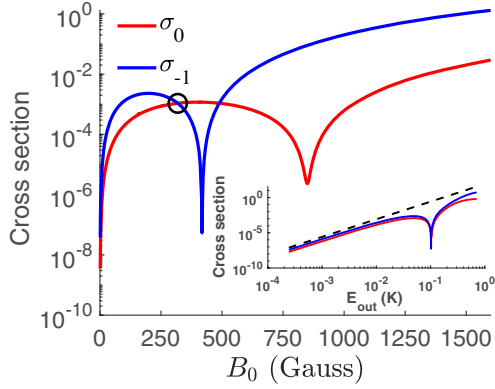


FIG. 3. ${}^3\text{He} + {}^{17}\text{O}_2$ inelastic cross sections (in \AA^2) of the scattering channels $M_J = 1 \rightarrow M_J = 0$ (σ_0) and $M_J = 1 \rightarrow M_J = -1$ (σ_{-1}) as a function of static magnetic field strength B_0 with collision energy $E_{\text{in}} = 1 \mu\text{K}$. At the point marked by the black circle, the values of σ_0 and σ_{-1} are equal with $B_0 = 320 \text{ G}$. The inset shows the dependency of σ_0 , σ_{-1} on exit kinetic energy E_{out} , where the local minima of σ_0 and σ_{-1} are both achieved at $E_{\text{out}} = 0.1027 \text{ K}$. The dashed black line shows the $E_{\text{out}}^{5/2}$ scaling of the cross section.

cross sections of the two spin-flip channels, we have $\sigma_0 = \int_{-\infty}^{+\infty} F_0(E)G_0(E)dE = \sum_K |\lambda_{0,K}|^2 G_0(\hbar B_0 - K\omega_B)$ and $\sigma_{-1} = \int_{-\infty}^{+\infty} F_{-1}(E)G_{-1}(E)dE = \sum_L |\lambda_{-1,L}|^2 G_{-1}(2\hbar B_0 - L\omega_B)$, where $G_0 = 2\pi|g_0|^2/I$, $G_{-1} = 2\pi|g_{-1}|^2/I$ and I is the incident flux (rigorous expressions of G_0 , G_{-1} using MFF-CC theory are given in the Supplemental Material [33]). Figure 3 shows the inelastic cross sections as a function of static magnetic field at $E_{\text{in}} = 1 \mu\text{K}$ with the potential calculated by the Møller-Plesset perturbation theory [20]. The sharp minima of the cross sections arise from interference between the incident s and emergent d radial wave functions in the inelastic scattering [20]. The cross section minima in ultracold scattering exist in various atomic and molecular processes [13,35,36].

In order to obtain $G_0(E_{\text{out}})$ and $G_{-1}(E_{\text{out}})$, we used series of trial magnetic pulses to calculate the Fourier coefficients $\lambda_{0,K}$ and $\lambda_{-1,L}$. And by applying the multifrequency Floquet coupled channel algorithm, we calculated the inelastic cross sections $\sigma_{0,K}$ and $\sigma_{-1,L}$ numerically. Using the relationships $G_0(\hbar B_0 - K\omega_B) = \sigma_{0,K}/|\lambda_{0,K}|^2$ and $G_{-1}(2\hbar B_0 - L\omega_B) = \sigma_{-1,L}/|\lambda_{-1,L}|^2$, we retrieve the values of $G_0(\hbar B_0 - K\omega_B)$ and $G_{-1}(2\hbar B_0 - L\omega_B)$. In particular, when only the static magnetic field B_0 is applied, we obtain $\varepsilon_0(t) = \varepsilon_{-1}(t) = 1$ and $\sigma_0 = G_0(\hbar B_0)$, $\sigma_{-1} = G_{-1}(2\hbar B_0)$. Figure 4 illustrates the calculated transition probabilities $G_f(E_{\text{out}})$ at $E_{\text{in}} = 1 \mu\text{K}$. Within the range of the collision energy and the magnetic field considered here, the inelastic scattering is dominated by the s partial wave, and the spin-flip transitions require boosting the angular momentum from $l = 0$ to $l = 2$. Since the centrifugal barrier of $\sim 0.59 \text{ K}$ for the d partial wave in the exit channel is much larger than E_{out} , Wigner's threshold law is well reflected by the threshold behavior

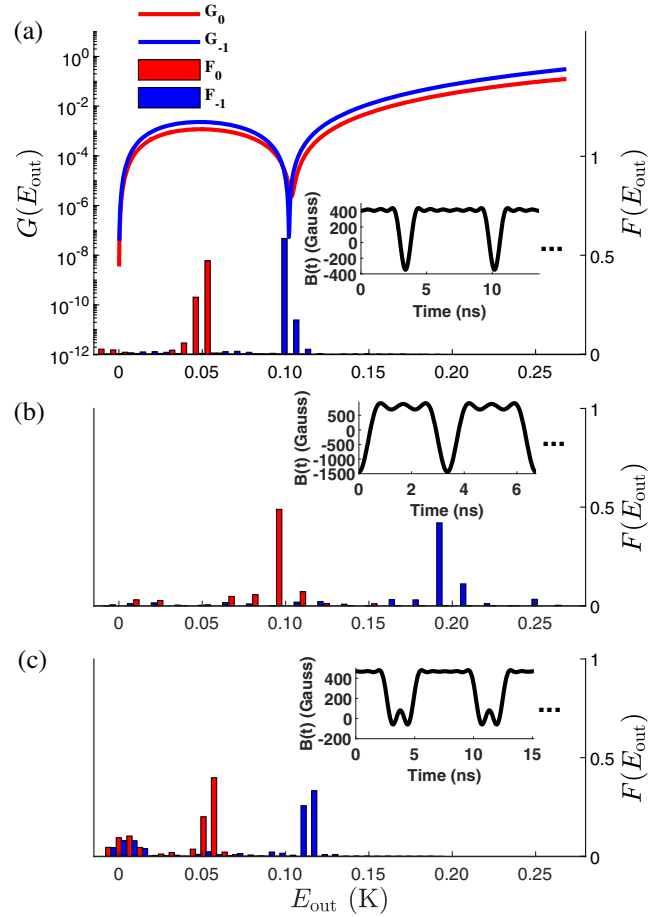


FIG. 4. Transition probabilities as a function of the exit kinetic energy E_{out} for the scattering channels $M_J = 1 \rightarrow M_J = 0$ (G_0) and $M_J = 1 \rightarrow M_J = -1$ (G_{-1}). Notice that the values of $G_0(\hbar B_0)$ and $G_{-1}(2\hbar B_0)$ are equal to σ_0 and σ_{-1} , respectively, when only the static field B_0 is applied. In order to select one channel, we choose a time-varying field $B(t) = B_0 + \mathcal{B}(t)$, where $B_0 = 320 \text{ G}$ and the specific form of $\mathcal{B}(t)$ is given in the main text, to concentrate $F_0(E_{\text{out}})$ or $F_{-1}(E_{\text{out}})$ around the minimum. The inset depicts two pulses of the pulse train $B(t)$ in time domain. (a) Selection of the $M_J = 1 \rightarrow M_J = 0$ channel, with $\sigma_0/\sigma_{-1} = 5.16$. (b) Selection of the $M_J = 1 \rightarrow M_J = -1$ channel, with $\sigma_{-1}/\sigma_0 = 209.42$. (c) Suppression of both channels. Here σ_0 , σ_{-1} are suppressed to 73%, 50%, respectively.

of transition probabilities, that G_0 and G_{-1} are proportional to $(E_{\text{out}})^{5/2}$ [20].

By tuning the time-dependent part of the magnetic field $\mathcal{B}(t)$ and keeping B_0 constant, we can dramatically vary the scattering cross sections of different channels and select the final states. The selection of different scattering channels can be easily implemented by concentrating the channel resolved spectral function $F_0(E_{\text{out}})$ [or $F_{-1}(E_{\text{out}})$] around the valley of corresponding transition probabilities $G_0(E_{\text{out}})$ [or $G_{-1}(E_{\text{out}})$], and the scattering cross section of $M_J = 1 \rightarrow M_J = 0$ or $M_J = 1 \rightarrow M_J = -1$ will be effectively suppressed. In order to facilitate the comparison, we choose $B_0 = 320 \text{ G}$ such that the cross sections

$\sigma_0 = 1.0813 \times 10^{-3} \text{ \AA}^2$, $\sigma_{-1} = 1.0601 \times 10^{-3} \text{ \AA}^2$ are approximately equal when only the static field is applied. Taking the fundamental frequency ω_B and amplitude a_n of the time varying part of magnetic field $\mathcal{B}(t)$ as variables and $\int_{-\infty}^{+\infty} F_f(E)G_f(E)dE$ as the objective function, we use a genetic algorithm to find the optimal magnetic field to suppress one of the scattering channels. To suppress the $M_J = 1 \rightarrow M_J = -1$ channel, the optimized field has $\omega_B = 2\pi \times 147.46 \text{ MHz}$, $a_1 = 184.40 \text{ G}$, $a_2 = -165.31 \text{ G}$, $a_3 = 132.02 \text{ G}$, $a_4 = -95.21 \text{ G}$, $a_5 = 59.59 \text{ G}$, and $a_6 = -30.52 \text{ G}$. The channel resolved spectral modulation functions $F_0(E_{\text{out}})$ and $F_{-1}(E_{\text{out}})$ are plotted in Fig. 4(a). The channel resolved cross sections are $\sigma_0 = 9.7835 \times 10^{-4} \text{ \AA}^2$, $\sigma_{-1} = 1.8959 \times 10^{-4} \text{ \AA}^2$, and σ_0 is about 5 times as large as σ_{-1} . To suppress the other channel $M_J = 1 \rightarrow M_J = 0$, the optimized field has $\omega_B = 2\pi \times 297.41 \text{ MHz}$, $a_1 = -853.72 \text{ G}$, $a_2 = -595.55 \text{ G}$, $a_3 = -312.67 \text{ G}$, and the spectral modulation functions are plotted in Fig. 4(b). The magnitude of the cross sections become $\sigma_0 = 2.2945 \times 10^{-4}$ and $\sigma_{-1} = 4.8051 \times 10^{-2} \text{ \AA}^2$, and σ_{-1} is 2 orders of magnitude larger than σ_0 . Furthermore, the scattering of both channels can be simultaneously suppressed by a suitable magnetic field. If we set $\omega_B = 2\pi \times 132.21 \text{ MHz}$, $a_1 = 245.66 \text{ G}$, $a_2 = -126.20 \text{ G}$, $a_3 = 6.71 \text{ G}$, $a_4 = 57.43 \text{ G}$, $a_5 = -57.57 \text{ G}$, $a_6 = 24.90 \text{ G}$, the cross sections become $\sigma_0 = 7.9059 \times 10^{-4}$ and $\sigma_{-1} = 5.3488 \times 10^{-4} \text{ \AA}^2$, which indicates scattering rates of the two channels are suppressed to 73% and 50%, respectively.

Though the collision energy E_{in} has a Maxwellian distribution, the shapes of $G_0(E_{\text{out}})$ and $G_{-1}(E_{\text{out}})$ are almost independent of E_{in} for ultracold collision, hence our control scheme is robust for a thermal distribution of the incident kinetic energy under this circumstance (see explanation in the Supplemental Material [33]). Notice that $^{17}\text{O}_2$ has no permanent dipole moment, whereas the magnitude of permanent quadrupole is $10^{-40} \text{ C} \cdot \text{m}^2$ [37], the polarizability induced by the transition dipoles is about $10^{-40} \text{ C} \cdot \text{m}^2/\text{V}$ [38], and the $\text{O}_2\text{-He}$ complex has a dipole of about 10^{-3} D [39]. Although the time-dependent magnetic field can generate electric field, the total energy shift (less than 0.1 MHz) due to the Stark effect is much smaller than the Zeeman splitting and Floquet level spacing, thus we only need to consider the effect of magnetic field.

In conclusion, we have introduced a theoretical method for solving the quantum scattering problem in the presence of a pulsed external field based on the multifrequency Floquet approach, and demonstrated flexible tuning of inelastic scattering cross sections by a magnetic pulse train. We realize effective selection of scattering channels, which can be interpreted as a selective quantum Zeno effect. Existing experimental techniques in ultracold scattering experiments [15,17,23,40–43] can be employed to realize the channel selection with a time-dependent

magnetic field. The method in this work can be directly applied to control broad types of multichannel inelastic and reactive scattering processes with time-dependent magnetic, microwave, and laser fields of complex temporal structure.

The authors are thankful to G. Chałasiński for helpful discussions. This work was supported by the National Natural Science Foundation of China (No. 12174009, No. 11974031, No. 12104082). J. L. B. acknowledges the support from the National Science Foundation under Grant No. PHY 1734006.

^{*}These authors contributed equally to this work.

[†]gaoren.wang@dlut.edu.cn

[‡]xuht@sustech.edu.cn

[§]zheng.li@pku.edu.cn

- [1] A. G. Kofman and G. Kurizki, *Phys. Rev. Lett.* **87**, 270405 (2001).
- [2] G. Kurizki and A. G. Kofman, *Nature (London)* **405**, 546 (2000).
- [3] P. Facchi and S. Pascazio, *Phys. Rev. Lett.* **89**, 080401 (2002).
- [4] P. Facchi, D. A. Lidar, and S. Pascazio, *Phys. Rev. A* **69**, 032314 (2004).
- [5] X. Guo, C.-L. Zou, L. Jiang, and H. X. Tang, *Phys. Rev. Lett.* **120**, 203902 (2018).
- [6] F. Dreisow, A. Szameit, M. Heinrich, T. Pertsch, S. Nolte, A. Tünnermann, and S. Longhi, *Phys. Rev. Lett.* **101**, 143602 (2008).
- [7] G. Barontini, L. Hohmann, F. Haas, J. Estève, and J. Reichel, *Science* **349**, 1317 (2015).
- [8] L. Bretheau, P. Campagne-Ibarcq, E. Flurin, F. Mallet, and B. Huard, *Science* **348**, 776 (2015).
- [9] G. A. Paz-Silva, A. T. Rezakhani, J. M. Dominy, and D. A. Lidar, *Phys. Rev. Lett.* **108**, 080501 (2012).
- [10] R. N. Zare, *Science* **279**, 1875 (1998).
- [11] R. V. Krems, *Phys. Rev. Lett.* **96**, 123202 (2006).
- [12] T. V. Tscherbul and R. V. Krems, *Phys. Rev. Lett.* **115**, 023201 (2015).
- [13] T. V. Tscherbul and R. V. Krems, *Phys. Rev. Lett.* **97**, 083201 (2006).
- [14] M. Shapiro and P. Brumer, *Quantum Control of Molecular Processes* (Wiley-VCH, New York, 2012).
- [15] J. R. Li, W. G. Tobias, K. Matsuda, C. Miller, G. Valtolina, L. De Marco, R. R. W. Wang, L. Lassabliere, G. Quemener, J. L. Bohn, and J. Ye, *Nat. Phys.* **17**, 1144 (2021).
- [16] L. Anderegg, S. Burchesky, Y. Bao, S. S. Yu, T. Karman, E. Chae, K.-K. Ni, W. Ketterle, and J. M. Doyle, *Science* **373**, 779 (2021).
- [17] X. He, K. Wang, J. Zhuang, P. Xu, X. Gao, R. Guo, C. Sheng, M. Liu, J. Wang, J. Li, G. V. Shlyapnikov, and M. Zhan, *Science* **370**, 331 (2020).
- [18] Z. Zhang, L. Chen, K.-X. Yao, and C. Chin, *Nature (London)* **592**, 708 (2021).
- [19] Y. Liu, M.-G. Hu, M. A. Nichols, D. Yang, D. Xie, H. Guo, and K.-K. Ni, *Nature (London)* **593**, 379 (2021).
- [20] A. Volpi and J. L. Bohn, *Phys. Rev. A* **65**, 052712 (2002).

- [21] M. L. González-Martínez and J. M. Hutson, *Phys. Rev. A* **75**, 022702 (2007).
- [22] T. V. Tscherbul, Y. V. Suleimanov, V. Aquilanti, and R. V. Krems, *New J. Phys.* **11**, 055021 (2009).
- [23] W. C. Campbell, E. Tsikata, Hsin-I. Lu, L. D. van Buuren, and J. M. Doyle, *Phys. Rev. Lett.* **98**, 213001 (2007).
- [24] A. O. G. Wallis and J. M. Hutson, *Phys. Rev. Lett.* **103**, 183201 (2009).
- [25] A. Devolder, P. Brumer, and T. V. Tscherbul, *Phys. Rev. Lett.* **126**, 153403 (2021).
- [26] L. Zhou, S. Yang, Y.-X. Liu, C. P. Sun, and F. Nori, *Phys. Rev. A* **80**, 062109 (2009).
- [27] C. Langmack, D. H. Smith, and E. Braaten, *Phys. Rev. Lett.* **114**, 103002 (2015).
- [28] D. H. Smith, *Phys. Rev. Lett.* **115**, 193002 (2015).
- [29] R. Zhang, Y. Cheng, H. Zhai, and P. Zhang, *Phys. Rev. Lett.* **115**, 135301 (2015).
- [30] J. L. Roberts, N. R. Claussen, S. L. Cornish, and C. E. Wieman, *Phys. Rev. Lett.* **85**, 728 (2000).
- [31] R. V. Krems and A. Dalgarno, *J. Chem. Phys.* **120**, 2296 (2004).
- [32] R. V. Krems, *Molecules in Electromagnetic Fields: From Ultracold Physics to Controlled Chemistry* (John Wiley & Sons, New York, 2018).
- [33] See Supplemental Material at <http://link.aps.org/supplemental/10.1103/PhysRevLett.129.013402> for the multifrequency Floquet theory, the calculation of scattering rates, the derivation of transition probabilities, and the impact of thermal distribution.
- [34] E. W. Streed, J. Mun, M. Boyd, G. K. Campbell, P. Medley, W. Ketterle, and D. E. Pritchard, *Phys. Rev. Lett.* **97**, 260402 (2006).
- [35] J. M. Hutson, M. Beyene, and M. L. González-Martínez, *Phys. Rev. Lett.* **103**, 163201 (2009).
- [36] T. Sikorsky, M. Morita, Z. Meir, A. A. Buchachenko, R. Ben-shlomi, N. Akerman, E. Narevicius, T. V. Tscherbul, and R. Ozeri, *Phys. Rev. Lett.* **121**, 173402 (2018).
- [37] V. W. Couling and S. S. Ntombela, *Chem. Phys. Lett.* **614**, 41 (2014).
- [38] D. Spelsberg and W. Meyer, *J. Chem. Phys.* **101**, 1282 (1994).
- [39] B. F. Minaev and G. Kobzev, *Spectrochim. Acta Part A* **59**, 3387 (2003).
- [40] S. T. Thompson, E. Hodby, and C. E. Wieman, *Phys. Rev. Lett.* **95**, 190404 (2005).
- [41] S. Aubin, S. Myrskog, M. H. T. Extavour, L. J. LeBlanc, D. McKay, A. Stummer, and J. H. Thywissen, *Nat. Phys.* **2**, 384 (2006).
- [42] E. A. Donley, N. R. Claussen, S. T. Thompson, and C. E. Wieman, *Nature (London)* **417**, 529 (2002).
- [43] N. Akerman, M. Karpov, Y. Segev, N. Bibelnik, J. Narevicius, and E. Narevicius, *Phys. Rev. Lett.* **119**, 073204 (2017).